# Band offsets between $ZnGeN_2$, GaN, ZnO, and $ZnSnN_2$ and their potential impact for solar cells

Atchara Punya and Walter R. L. Lambrecht
*Department of Physics, Case Western Reserve University, Cleveland, Ohio 44106-7079, USA*
(Received 15 May 2013; published 2 August 2013)

The band offsets between the Zn-IV-$N_2$ nitrides, $ZnGeN_2$ and $ZnSnN_2$, and two other closely lattice matched semiconductors, ZnO and GaN, are calculated using density functional theory calculations including quasiparticle corrections. The interface dependence as well as the role of strain are investigated. A staggered type-II alignment is found between $ZnGeN_2$, GaN, and ZnO, with ZnO having the lower and $ZnGeN_2$ having the higher valence band maximum. The potential benefits of this alignment for photovoltaic applications are pointed out.

DOI: 10.1103/PhysRevB.88.075302 PACS number(s): 31.15.E−, 73.22.−f, 73.40.−c

## I. INTRODUCTION

Band offsets at heterojunctions play an important role in semiconductor devices, such as light emitting diodes (LED) and solar cells. They lead to built-in electric fields which allow one to control the spatial distribution of carriers. For an LED, carrier confinement of both holes and electrons in the same region is beneficial, while for photovoltaic applications, separation of photogenerated electrons and holes is required. Recently, some new nitride semiconductors have become of interest besides the already well-studied group-III nitrides.[1–3] In these new heterovalent nitrides with composition II-IV-$N_2$, the four group-III cations surrounding each nitrogen are replaced by two group-II and two group-IV ions, e.g., $ZnGeN_2$ instead of GaN. In a recent paper, we presented electronic band structures for Zn-IV-$N_2$ semiconductors.[3] Several papers have recently appeared[4–6] on the growth of $ZnSnN_2$ and pointed out the opportunities of this material for photovoltaics based on earth-abundant elements because of its relatively low band gap, estimated in different papers between 1.4 and 2.0 eV. Our own best estimate based on the quasiparticle self-consistent $GW$ method and using the experimental lattice constant is $1.8 \pm 0.1$ eV. This differs slightly from the value given in Ref. 3 because in that paper we had used the slightly underestimated local density approximation (LDA) lattice constants, while the present value corresponds to the experimental lattice constants of Ref. 6 at room temperature. While $ZnGeN_2$ has a gap of 3.4 eV,[3,7] which is far from optimal for photovoltaic applications, we point out here the interesting opportunity that $ZnGeN_2$, wurtzite GaN, and ZnO have all three almost equal band gap of ∼3.4 eV and are closely lattice matched. This means necessarily that the band offsets must be staggered or so-called type II. Throughout this paper, we assume the wurtzite structures for ZnO and GaN as these are the lowest-energy structures. This creates a situation where an effectively smaller band gap exists across the interface. This leads to the possibility of absorption at lower photon energies and effective separation of electrons and holes in the different semiconductors joined at the interface. The questions are as follows: How large are the band offsets between these materials? Do they lead to effective absorption in the visible range? We will show in this paper that if the materials are arranged from low to high valence band maximum (VBM), the valence band offsets are from 0.4–2.6 eV, thus predicting significantly lower effective gaps at the interfaces.

This is of interest from a fundamental point of view because it highlights the role of Zn-3$d$ orbitals and the anion in affecting the valence band maximum. $ZnGeN_2$, GaN, and ZnO indeed differ in that in $ZnGeN_2$, the Zn-3$d$ electrons lie at about 7 eV below the VBM, whereas the Ga-3$d$ states lie about 17 eV below the VBM. In ZnO, on the other hand, we have even shallower Zn-3$d$ levels at about 6 eV, but now the anion O-2$p$ states are also deeper than N-2$p$ states.

We exclude $ZnSiN_2$ from this study because it has an indirect gap and a larger lattice mismatch from the other materials. We include $ZnSnN_2$ although it has a larger lattice constant than the other three materials because it has been viewed as a potentially useful material for solar cells. Band offsets between group-III nitrides have been studied before[8] as well as between GaN and ZnO.[9–14]

## II. COMPUTATIONAL METHOD

Our calculations of the structure and electrostatic potential at the interfaces are based on the density functional theory[15,16] in the local density approximation. We use the full-potential linearized muffin-tin orbital method as band-structure method.[17,18] However, our calculation of the band structures themselves in each bulk material is based on the quasiparticle self-consistent (QS) $GW$ approach. Here, $G$ and $W$ stand for the one-particle Green's function and screened Coulomb interaction respectively, and $iGW$ is an approximation for the self-energy $\Sigma$.[19,20] This method is known to provide not only much improved band gaps, but also shifts of the individual band edges relative to the average electrostatic potential in each material. The QS$GW$ method actually overestimates gaps slightly because of the underestimate of the dielectric screening when neglecting electron-hole interaction effects. This is typically an effect of order 20% and, hence, reducing the QS$GW$ self-energy correction to 80% of its value, a more accurate result is obtained. Following, when we say QS$GW$ results, we actually mean that this 80% reduction effect has been included.

We calculate the alignment of the electrostatic potential using the LDA with a supercell approach for modeling the interface. The position of the bands relative to the potential is determined separately for each material including quasiparticle self-energy effects of the individual band edges. The band offsets are also strongly influenced by strain and depend on the particular arrangement at the heterostructure, the degree of epitaxy, etc. We first study coherently strained

 

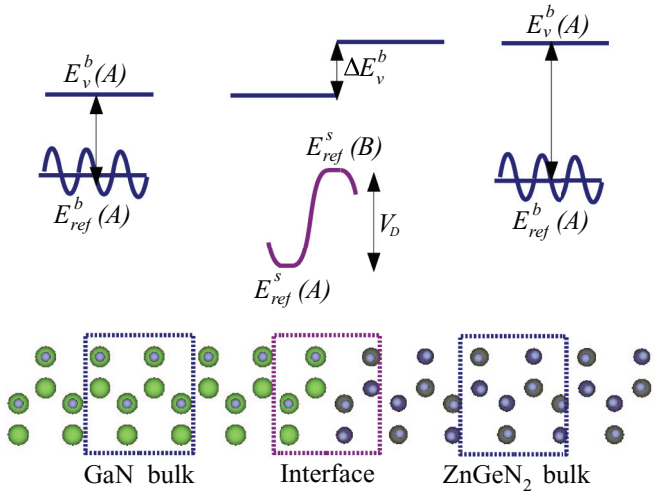


FIG. 1. (Color online) Diagram illustrating band-offset calculation procedure. The top part shows the difference between bulk band edges measured from the average electrostatic potential in each material and the interface dipole. The bottom part shows the positions of the atoms in the supercell and the identification of the two bulk regions inside it.

interfaces. We assume that the in-plane lattice constant is dictated by the substrate, and relax the distance perpendicular to the interface based on continuum elastic theory. The internal positions of the atoms and the interface layer separations are determined by relaxing the total energy. Deviations from the specific structural models or strain situations handled explicitly here can (if required) be analyzed later in terms of the deformation potential induced changes to the VBM for each individual material. We study the importance of these effects by examining three different interface orientations. We then attempt to extract from this an average interface-independent and strain-free "natural" band offset which might apply to more random situations, for example, an array of nanoparticles in close contact with different interfaces.

The procedure is illustrated in Fig. 1. The band offset is thus essentially separated in a bulk and interface contribution:

$$\begin{aligned}\Delta E_v(A/B) &= \left[E_v^b(B) - E_{\rm ref}^b(B)\right] - \left[E_v^b(A) - E_{\rm ref}^b(A)\right] \\ &\quad + \left[E_{\rm ref}^s(B) - E_{\rm ref}^s(A)\right] \\ &\equiv \Delta E_v^b + V_D. \end{aligned} \tag{1}$$

The first two terms give the bulk valence band maximum relative to some suitable reference level in each material separately, and the third term gives the change in reference level across the interface. We call it the dipole potential $V_D$.[21] Several types of reference levels can be used.

All it needs is some suitable markers of the potential in the materials that can be identified in the separate bulk as well as locally in the interface system whose potential can be viewed as being bulklike during the layers sufficiently far from the interface, except for a constant shift near the interface. In practice, for example, it is common for experimentalists to use a core level as reference level. Here, we use the average potential at the muffin radius over the atoms in a layer. The average is taken weighted by the area of the spheres

$$\overline{V} = \frac{\sum_i V_i s_i^2}{\sum_i s_i^2}. \tag{2}$$

Here, $V_i$ is the potential at the sphere radius $s_i$ of the $i$th muffin-tin sphere and the sum is over all atoms in a given atomic layer.

It is convenient to focus first on nonpolar directions such as the [100] and [010] directions. In this case, each layer is neutral in bulk. For the polar direction [001], because of the difference in spontaneous polarization, and the piezoelectric polarization due to the specific strain, a net charge can occur at the interface and this leads to an overall electric field in each different semiconductor region, in other words, a sloped potential. This slope is then superposed on the dipolar shift that occurs also over a few atomic layers and this makes it a little more ambiguous to separate the in-principle abrupt dipole jump and slope discontinuity. In a previous paper,[2] we have shown that the spontaneous polarization of $ZnGeN_2$, GaN, and $ZnSnN_2$ are relatively close to each other, so that these effects are small, although they may be somewhat larger for the interfaces with ZnO. In reality, the surface charge resulting form the discontinuity in polarization $\sigma = \Delta P \cdot \hat{n}$, which in a continuum model is a strict two-dimensional (2D) charge per unit area, is distributed over some layers, and thus the potential is not really discontinuous in slope. The dipole discontinuity is likewise not abrupt at the atomic scale and this results in some difficulty in disentangling the two from each other.

So, to summarize, we set up a suitable supercell, modeling the interface with a few layers of each material, and calculate its self-consistent potential. Then, we apply the above filtering and averaging procedure to extract the interface dipole profile and extract from this the $V_D$ term. The band edges with respect to the same type of average are determined separately in each material also within the local density approximation. However, a quasiparticle correction for each material is then applied to the band edges relative to the electrostatic potential. In other words, we take into account how much each band edge is shifted from its LDA to its $GW$ result relative to the same electrostatic potential average. As discussed earlier,[3] this makes sense within the quasiparticle self-consistent $GW$ method, in which our Kohn-Sham eigenvalues approach the quasiparticle energies once the exchange correlation potential is self-consistently determined from the $GW$ self-energy.

Our assumptions for a specific strain state assume one of the materials, say GaN, is the substrate. We then adjust $ZnGeN_2$ to be biaxially strained to the substrate, i.e., to have the same in-plane lattice constants as the substrate. The perpendicular lattice constant is obtained by minimizing the strain energy

$$U = \frac{1}{2}(\eta_1, \eta_2 \eta_3) \begin{pmatrix} c_{11} & c_{12} & c_{13} \\ c_{12} & c_{22} & c_{23} \\ c_{13} & c_{23} & c_{33} \end{pmatrix} \begin{pmatrix} \eta_1 \\ \eta_2 \\ \eta_3 \end{pmatrix} \tag{3}$$

using the previously calculated elastic constants.[2] For the interface layer separation, we initially assume the average of the two bulk interplanar distances and this sets the overall lattice constants of the supercell. Afterwards, all atomic positions as well as the interface layer separation (or equivalently, the overall lattice constant in the direction perpendicular to the

interface) are relaxed to minimize the total energy. We find that this results primarily in adjustment of the interlayer separations right next to the interface.

The bulk contribution $\Delta E_v^b$ is calculated with the appropriately strained separate materials as occurring at the interface. It can be decomposed into an unstrained contribution $\Delta E_v^0$ and a strain contribution: $\Delta E_v^b = \Delta E_v^0 + \Delta_s$. To evaluate the importance of the $GW$ correction, we further decompose $\Delta E_v^0$ into the LDA part and its $GW$ correction $\Delta E_v^0(GW) = \Delta E_v^0(\mathrm{LDA}) + \Delta_{GW}$. In fact, these contributions can be given separately for each material, but the strain contribution depends on which strain situation is considered, and hence on the interface. Note that the strain here is biaxial and contains both a traceless as well as a hydrostatic component. The hydrostatic absolute deformation potential requires itself an interface calculation between unstrained and strained material because the reference level is not guaranteed to be the same between two separate bulk calculations. We have checked with separate calculations of strained $ZnGeN_2$ on unstrained $ZnGeN_2$ that this effect is less than 0.1 eV on the $\Delta_s$. By comparing the strained with the unstrained bulk $ZnGeN_2$, we can undo the strain effect to extract a "natural" band offset, i.e., $\Delta E_v^{\mathrm{nat}} = \Delta E_v^0 + \bar{V}_D$, where the average of $V_D$ over different orientations is indicated by $\bar{V}_D$.

This would, for example, occur if we assume that the $ZnGeN_2$ is too thick to stay pseudomorphic and instead relaxes by introducing misfit dislocations. We have no way currently to take into account the effects of those misfit dislocations on the dipole, but we can easily estimate the changes in band edges due to the different strain states in the bulk. In principle, some other residual strain state might occur due to thermal expansion mismatch. For example, it is common to assume that at the growth temperature, the film is fully relaxed but after cooling a strain results from the different thermal expansion coefficients. Once we have a natural strain-free band offset, it would in principle be possible to add strain effects in terms of deformation potentials assuming the strain state is known or measured for a specific situation. For GaN/$ZnGeN_2$, these effects are all expected to be rather small.

## III. RESULTS

We start by illustrating the methodology for the GaN/$ZnGeN_2$ case. Figure 2 shows the average potentials as discussed in the previous section for three different interface orientations and the dipole potential $V_D$ extracted from them. We used supercells consisting of four (or six) layers of GaN and four (or six) layers of $ZnGeN_2$. Only the results for the larger cells are shown in Fig. 2. The dipoles extracted from the smaller cells agree with the larger ones within 0.1 eV and, therefore, for the other materials, we have used the smaller cells. The lattice constants obtained by minimizing the strain for the $ZnGeN_2$ region for each interface are summarized in Table I and compared with the equilibrium lattice constants of unstrained $ZnGeN_2$ and GaN.

The separation of the valence band edges relative to the average electrostatic potential in the LDA, its $GW$ correction, and the band gap for each material are given in Table II. The band gap given here is the low-temperature experimental exciton gap rounded to 0.1 eV, which agrees well with QS$GW$

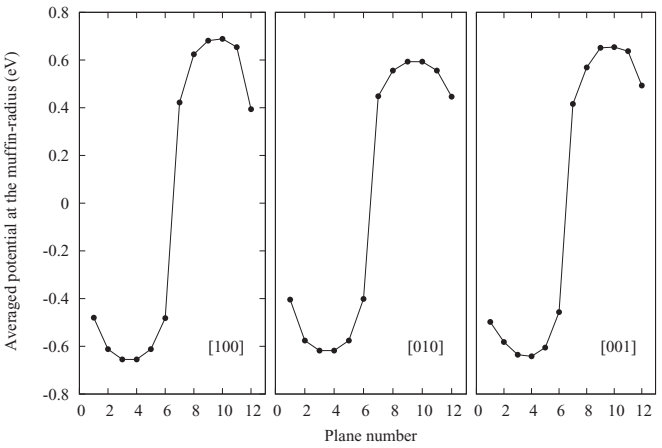


FIG. 2. Potential profiles for different interfaces for GaN/$ZnGeN_2$. The potential shown is the $\bar{V}$ of Eq. (2).

after the $0.8\Sigma$ correction, a zero-point motion and exciton binding-energy correction.[3]

The extracted dipole potentials $V_D$ and $\Delta E_v^b$ including the strain effects are included in Table III for each pair of interfaces calculated directly. The average over directions is also included.

In Fig. 3, we show the total densities of states (DOS), resolved layer by layer. One could in principle read off the band offsets directly from this figure by taking the difference between the VBM in the central layers in each half of the unit cell. However, the procedure discussed before is somewhat more accurate. The two are, in fact, in good agreement. The total DOS illustrates that the middle layers are indeed already bulklike, in other words, that our supercell is large enough.

We can see that the band offsets between $ZnGeN_2$ and GaN depend only little on the interface direction. The variation is only 0.08 eV. This is because the materials are the closest lattice matched. For the other cases, the strain effects are somewhat larger and hence also the band-offset variation with interface orientation. By leaving out the strain contribution, we obtain an estimate of strain relaxed instead of coherently strained interfaces. The average of these over the three interfaces is what we defined as a "natural" band offset.

Finally, we summarize the valence as well as conduction band offsets and gap discontinuities in Table IV not only for the pairs directly calculated, but also the other ones, which follows from the transitivity rule. We can see that all heterostructures considered have a type-II alignment, except for $ZnGeN_2$/$ZnSnN_2$. For all type-II heterostructures, the

TABLE I. Orthorhombic structure lattice constants as strained for particular GaN/$ZnGeN_2$ interfaces.

| | $a$ (Å) | $b$ (Å) | $c$ (Å) |
|---|---|---|---|
| $ZnGeN_2$ (unstrained bulk) | 6.38 | 5.45 | 5.22 |
| $ZnGeN_2$ [100] | 6.40 | 5.47 | 5.14 |
| $ZnGeN_2$ [010] | 6.31 | 5.49 | 5.14 |
| $ZnGeN_2$ [001] | 6.31 | 5.47 | 5.31 |
| GaN (unstrained substrate) | 6.31 | 5.47 | 5.14 |

TABLE II. Decomposition of band edge [relative to average electrostatic potential $\bar{V}$ as defined in Eq. (2)] in each material in LDA, its $GW$ shift, and band gap (units in eV).

| | $E_v^0$ (LDA) | $\Delta_{GW}$ | $E_g$ |
|---|---|---|---|
| GaN | 9.30 | −0.34 | 3.5 |
| $ZnGeN_2$ | 9.40 | −0.13 | 3.4 |
| $ZnSnN_2$ | 10.42 | 0.20 | 1.8 |
| ZnO | 6.45 | −1.62 | 3.4 |

lowest gap of the overall system is between the VBM of one and the CBM of the other material. This transition is spatially indirect and therefore we expect optical absorption at this smallest gap only near the interface. We therefore call it "the interface gap" $E_g^{i,av}$, average ($av$) meaning with respect to different interface directions. It is included in Table IV. On the other hand, $ZnGeN_2$ has a type-I alignment with $ZnSnN_2$, which means that $ZnSnN_2$ quantum wells could be created with $ZnGeN_2$ barriers for LED type of applications. The alignments of the valence bands and conduction bands between all four materials are also conveniently summarized in Fig. 4. The interface gaps as well as the valence and conduction band offsets of each pair can be directly read from this figure.

Considering the three materials with gaps near 3.4 eV, we note that the valence band offsets are of order 1–2 eV and we find the VBMs ordered from low to high from ZnO to $ZnGeN_2$. This would imply that electrons will migrate from $ZnGeN_2$ to GaN to ZnO if all three were present in the same structure. Holes, on the other hand, will migrate from ZnO to GaN to $ZnGeN_2$. This separation of carriers of different polarity in different regions is advantageous for photovoltaic applications. While the band gaps of these materials are in the UV and hence not directly suitable for terrestrial solar-cell applications, one may expect light absorption at the smaller effective interface gap of these heterostructures. This could be significant if a major portion of the material is near the interfaces, in other words, if it is nanostructured. These occur at 1.2 eV (infrared) at the ZnO/$ZnGeN_2$ interface, 2.0 eV (yellow) at the GaN/$ZnGeN_2$ interface, and at 2.7 eV (blue) at the ZnO/GaN interface, thus covering various portions of the visible spectrum and the near infrared. We envision a solar cell of the type schematically shown in Fig. 5. It would consist of nanosize columns of each of the materials, arranged in such a way that all three interfaces occur between them. We caution that the effective band gaps in these heterostructures could be larger than the interface gaps given in Table IV because of the size-quantization effect. By further varying the sizes of these nanocolumns and hence their band gaps, one could further improve the range of wavelengths for which light absorption can take place. Including $ZnSnN_2$ in the design of such a solar cell would further allow absorption at 1.8 eV (red) and even further in the near IR (0.8 eV). We note that the VBM of $ZnSnN_2$ is the highest of the four materials, so ultimately holes would migrate to $ZnSnN_2$ while the conduction band of $ZnSnN_2$ is above those of ZnO and GaN, so electrons would still accumulate to ZnO. Of course, the growth of such a solar cell with well-separated materials and sharp interfaces presents a considerable challenge to thin-film and nanostructured growth method.

TABLE III. Dipole potentials and valence band offsets in each direction from eight-layer supercell (units in eV). (Values in parentheses are obtained from 12-layer supercell.)

| | GaN/$ZnGeN_2$ | ZnO/$ZnGeN_2$ | GaN/$ZnSnN_2$ |
|---|---|---|---|
| $\Delta E_v^0(GW)$ | 0.31 | 4.44 | 1.66 |
| $\Delta_s^{[100]}$ | 0.15 | 0.25 | 0.24 |
| $\Delta_s^{[010]}$ | 0.19 | 0.29 | 0.33 |
| $\Delta_s^{[001]}$ | 0.14 | 0.21 | 0.34 |
| $V_D^{[100]}$ | 1.15(1.29) | −2.21 | 0.18 |
| $V_D^{[010]}$ | 1.04(1.17) | −2.10 | 0.18 |
| $V_D^{[001]}$ | 1.10(1.24) | −2.43 | 0.23 |
| $\bar{V}_D$ | 1.10(1.23) | −2.25 | 0.20 |
| $\Delta E_v^{[100]}$ | 1.61(1.75) | 2.48 | 2.08 |
| $\Delta E_v^{[010]}$ | 1.54(1.67) | 2.63 | 2.17 |
| $\Delta E_v^{[001]}$ | 1.55(1.69) | 2.22 | 2.23 |

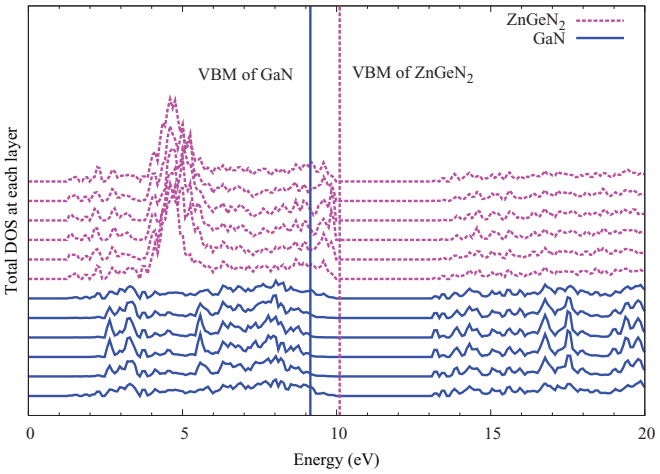


FIG. 3. (Color online) Total DOS at each layer of GaN/$ZnGeN_2$ heterostructure in the $Y$-interface direction.

## IV. DISCUSSION

The only case for which we are aware of previous results in the literature is the ZnO/GaN interface. Our valence band offset of 0.8 eV is in good agreement with the experimental results of Liu *et al.*[10] based on photoemission measurements of thin films of GaN grown on ZnO. They find $0.7 \pm 0.1$ eV

TABLE IV. Natural valence and conduction band offsets, gap differences, and effective interface gaps of heterostructures (in units of eV). (The values in parentheses correspond to the larger supercells.)

| | $\Delta E_v^{\text{nat}}$ | $\Delta E_c^{\text{nat}}$ | $\Delta E_g$ | $E_g^{i,av}$ |
|---|---|---|---|---|
| GaN/$ZnGeN_2$ | 1.4(1.5) | 1.3(1.4) | −0.1 | 2.1(2.0) |
| GaN/$ZnSnN_2$ | 1.9 | 0.2 | −1.7 | 1.6 |
| ZnO/GaN | 0.8(0.7) | 0.9(0.8) | 0.1 | 2.6(2.7) |
| ZnO/$ZnGeN_2$ | 2.2 | 2.2 | 0.0 | 1.2 |
| ZnO/$ZnSnN_2$ | 2.7(2.6) | 1.1(1.0) | −1.6 | 0.7(0.8) |
| $ZnGeN_2$/$ZnSnN_2$ | 0.5(0.4) | −1.1(−1.2) | −1.6 | |

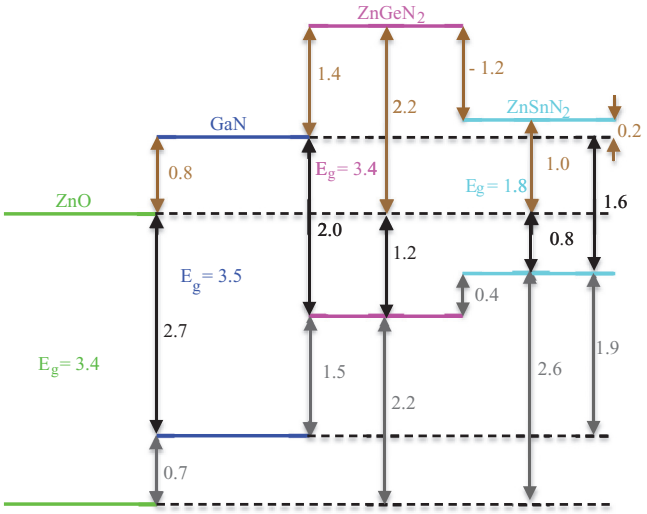


FIG. 4. (Color online) Natural band-offset alignment of ZnO, GaN, $ZnGeN_2$, and $ZnSnN_2$ and their effective interface gaps (in eV).

for polar and $0.9 \pm 0.1$ eV for nonpolar interfaces. On the other hand, Veal *et al.*[11] obtained the ZnO/GaN band offset of 1.37 eV in an indirect way by measuring the ZnO/AlN band offset and using the transitivity rule. McDermott *et al.*[13] studied mixed ZnO/GaN solid solution systems and proposed a 1.6-eV band offset between the ZnO and GaN phases in such systems. They found an effective gap of about 2.6–2.8 eV in such systems, in agreement with our proposed interface gap. However, the quantum size effects on the ZnO and GaN phases in such a mixed system are not completely clear. Their valence band offset is deduced from examining second derivatives of the O-K and N-K x-ray absorption and emission spectra in the mixed systems. They find evidence that such a mixed system is in fact phase separated at the nanoscale rather than forming a homogeneous superlattice oxynitride.

On the theory side, Huda *et al.*[12] found a band offset of 0.7 eV using the GGA + $U$ method, i.e., including a Hubbard $U$ for Ga 3$d$ and Zn 3$d$. Wang *et al.*[14] also calculated a valence band offset of 1.04 eV using GGA + $U$. They in addition studied core-shell nanowire heterostructures. Wang *et al.*[9] find valence band offsets ranging from 0.455 to 1.588 eV depending on which exchange correlation functional is used. Using GGA functionals PBE or PW91, they find relatively small offsets

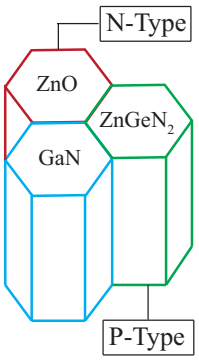


FIG. 5. (Color online) Concept of nanosize columnar solar cell of ZnO, GaN, and $ZnGeN_2$.

while adding Hubbard $U$ for the Zn 3$d$ and Ga 3$d$, the band offset is increased. Their highest band offset is found for the hybrid functional HSE06 (Heyd-Scuseria-Ernzerhof[22]) in which they used a different fraction of Hartree-Fock mixing for both materials, so as to adjust the gaps. It is well known that HSE06 tends to shift down the valence band maximum and apparently in their calculation this occurs stronger for ZnO than for GaN (maybe because of the larger Hartree-Fock fraction used). This illustrates that obtaining a correct quasiparticle shift of the individual band edges is important. We note (from Table II) that among the materials studied here, the $GW$ correction is the most negative in ZnO and shows relatively smaller variation among the nitrides. Since these band offsets also depend strongly on strain, a detailed comparison between different results requires considering which strain state was assumed. For example, the results of Wang *et al.*[9] correspond to a coherently strained interface. Since in strained GaN, the VBM is split, it increases the valence band offset. It can also be seen in Table III that the strain contribution is positive in all cases. Wang *et al.*[9] found that the dipole contribution is almost independent of the functional used. This supports our approach of calculating the dipole at the LDA level, while the individual band edges in each material require the use of the $GW$ corrections. Our valence band offset for ZnO/GaN is also in good agreement with the embedded cluster approach calculations of Walsh *et al.*[23] which use a hybrid functional in the quantum mechanically treated region. Our calculations have assumed perfect crystals except for strain effects. Point defects and cation disorder, especially in the ternary nitride, may affect their valence band offset.[24]

## V. CONCLUSIONS

We have studied the band alignment between $ZnGeN_2$, $ZnSnN_2$, GaN, and ZnO. Calculations were carried out for coherent [100], [010], [001] interfaces of three pairs of the materials, GaN/$ZnGeN_2$, GaN/$ZnSnN_2$, and ZnO/$ZnGeN_2$. By separating out the strain contribution, we also deduced an averaged natural band offset for strain-relaxed materials. The $GW$ corrections to the band offset were found to be important for interfaces involving ZnO because among these materials, it has a much larger downward valence band shift between LDA and $GW$ band edges.

The band offsets at the other three possible pairs are deduced from the transitivity rule. They show that except for $ZnGeN_2$/$ZnSnN_2$, all other heterostructures considered are of type II, which is promising for charge separation at such interfaces. The effective "interface gaps" of these materials are in the visible to near infrared making them much more attractive for photovoltaics than the individual materials, which have gaps in the UV except for $ZnSnN_2$. These materials' valence bands are in increasing order from ZnO to GaN to $ZnGeN_2$ to $ZnSnN_2$. Their conduction bands are in decreasing order from $ZnGeN_2$ to $ZnSnN_2$ to GaN to ZnO. Thus, in a composite system comprising all four materials, holes would flow to $ZnSnN_2$ and electrons to ZnO. A columnar nanosize solar-cell concept was presented for how potentially these band offsets could be utilized in photovoltaic cells.

**ACKNOWLEDGMENTS**

The work presented here was supported by NSF under Grant No. DMR-1104595. Calculation used the High Performance Computing Resource in the Core Facility for Advanced Research Computing at Case Western Reserve University and the Ohio Supercomputer Center.

[1]T. R. Paudel and W. R. L. Lambrecht, Phys. Rev. B **78**, 115204 (2008).
[2]T. R. Paudel and W. R. L. Lambrecht, Phys. Rev. B **79**, 245205 (2009).
[3]A. Punya, W. R. L. Lambrecht, and M. van Schilfgaarde, Phys. Rev. B **84**, 165204 (2011).
[4]N. Feldberg, B. Keen, J. D. Aldous, D. Scanlon, P. A. Stampe, R. Kennedy, R. Reeves, T. D. Veal, and S. Durbin, in *Photovoltaic Specialists Conference (PVSC)*, 2012 38th IEEE (IEEE, Washington, DC, 2012), pp. 002524–002527.
[5]L. Lahourcade, N. C. Coronel, K. T. Delaney, S. K. Shukla, N. A. Spaldin, and H. A. Atwater, Adv. Mater. **25**, 2562 (2013).
[6]P. C. Quayle, K. He, J. Shan, and K. Kash, MRS Commun. **First View**, 1 (2013).
[7]K. Du, C. Bekele, C. C. Hayman, J. C. Angus, P. Pirouz, and K. Kash, J. Cryst. Growth **310**, 1057 (2008).
[8]A. Schleife, F. Fuchs, C. Rodl, J. Furthmuller, and F. Bechstedt, Appl. Phys. Lett. **94**, 012104 (2009).
[9]Z. Wang, M. Zhao, X. Wang, Y. Xi, X. He, X. Liu, and S. Yan, Phys. Chem. Chem. Phys. **14**, 15693 (2012).
[10]J. W. Liu, A. Kobayashi, S. Toyoda, H. Kamada, A. Kikuchi, J. Ohta, H. Fujioka, H. Kumigashira, and M. Oshima, Phys. Status Solidi B **248**, 956 (2011).
[11]T. D. Veal, P. D. C. King, S. A. Hatfield, L. R. Bailey, C. F. McConville, B. Martel, J. C. Moreno, E. Frayssinet, F. Semond, and J. Zúñiga-Pérez, Appl. Phys. Lett. **93**, 202108 (2008).
[12]M. N. Huda, Y. Yan, S.-H. Wei, and M. M. Al-Jassim, Phys. Rev. B **78**, 195204 (2008).
[13]E. J. McDermott, E. Z. Kurmaev, T. D. Boyko, L. D. Finkelstein, R. J. Green, K. Maeda, K. Domen, and A. Moewes, J. Phys. Chem. C **116**, 7694 (2012).
[14]Z. Wang, Y. Fan, and M. Zhao, J. Appl. Phys. **108**, 123707 (2010).
[15]P. Hohenberg and W. Kohn, Phys. Rev. **136**, B864 (1964).
[16]W. Kohn and L. J. Sham, Phys. Rev. **140**, A1133 (1965).
[17]M. Methfessel, M. van Schilfgaarde, and R. A. Casali, in *Electronic Structure and Physical Properties of Solids. The Use of the LMTO Method*, Lecture Notes in Physics Vol. 535, edited by H. Dreyssé (Springer, Berlin, 2000), p. 114.
[18]T. Kotani and M. van Schilfgaarde, Phys. Rev. B **81**, 125117 (2010).
[19]M. van Schilfgaarde, T. Kotani, and S. Faleev, Phys. Rev. Lett. **96**, 226402 (2006).
[20]T. Kotani, M. van Schilfgaarde, and S. V. Faleev, Phys. Rev. B **76**, 165106 (2007).
[21]W. R. L. Lambrecht, B. Segall, and O. K. Andersen, Phys. Rev. B **41**, 2813 (1990).
[22]J. Heyd, G. E. Scuseria, and M. Ernzerhof, J. Chem. Phys. **124**, 219906 (2006).
[23]A. Walsh, C. R. A. Catlow, M. Miskufova, and A. A. Sokol, J. Phys.: Condens. Matter **23**, 334217 (2011).
[24]D. O. Scanlon and A. Walsh, Appl. Phys. Lett. **100**, 251911 (2012).